

Study of Resolution of VELO Test-Beam Telescope

Victoria Wright⁴, Paolo Bartalini¹, Jan Buytaert², Paula Collins², Hans Dijkstra², Olivier Dormond¹, Markus Elsing², Raymond Frei¹, Tjeed Ketel³, Sander Klaus³, Chris Parkes⁴, David Steele¹, Leonard Studer², Thomas Ruf², and Frederick Teubert².

Abstract

This note describes the systematic study made of the resolution of the LHCb VELO telescope used in the Autumn 99 test-beam. Measurements were made of the resolution for each region of both the LHCb R and Φ vertex detectors. The best value obtained for a $40\mu\text{m}$ pitch detector was $5.8 \pm 0.5 \mu\text{m}$, which is comparable to the $6.0 \mu\text{m}$ prediction of the Technical Proposal. At larger pitches, it was found that the resolutions deviate from those given in the Technical Proposal e.g. for an $80 \mu\text{m}$ detector a resolution of $15.4 \pm 0.3 \mu\text{m}$ is compared to the Technical Proposal value of $10 \mu\text{m}$.

¹ Institut de Physique des Hautes Energies, Batiment des Sciences Physiques, Université de Lausanne, CH-1015, Switzerland.

² CERN, CH-1203, Geneva 23, Switzerland.

³ Vrije Universiteit (VU), De Boelelaan 1079, NL-1007, MC Amsterdam, Holland.

⁴ Department of Physics, University of Liverpool, Oliver Lodge Laboratory, Oxford Street, Liverpool, L69 7ZE, UK.

Contents

1	Introduction	1
2	The LHCb VELO and Test-Beam Telescope	1
2.1	<i>R</i> and Φ Detectors	1
2.2	The Test-Beam Telescope	1
3	VELO Test-Beam Analysis Code	2
4	Telescope Resolution	2
4.1	Experimental Procedure	2
4.2	Analysis	3
4.3	Intrinsic Spatial Resolution	3
5	Conclusions and the Future	5
6	Acknowledgements	6

1 Introduction

This note describes the study of the first prototype detectors for the LHCb VERtEX LOcator. Data was taken during testing in the West Area (X7) at CERN in September 1999. The telescope, which is identical to that used in the Autumn 1998 test-beam, is described in further detail in section 2 along with a brief resume of the R and Φ vertex detectors themselves.

Also in the beam were a number of test detectors such as an irradiated VERtEX LOcator, similar to those in the telescope, and detectors fitted with the “new” SCTA chip. The results from testing these detectors will not be described in this note.

Section 3 describes the VELO test-beam analysis code, while section 4 presents results on detector resolution.

2 The LHCb VELO and Test-Beam Telescope

2.1 R and Φ Detectors

The LHCb VELO will consist of a number of stations of silicon discs. In the Technical Proposal [1], each disc comprises six sectors (each sector having approximately a 72° coverage). Each station will include a disc of both R and Φ measuring detectors, separated by typically 2-5 mm. Each detector covers a distance from 1 cm to 5 cm radially from the beam axis and the AC coupled strips of both detectors are read out via the routing lines found in the second metal layer.

The R measuring detector can be divided into four sections (as shown schematically in figure 1). The first two sections (0, 1) can be found within the first 1.8 cm as measured radially from the beam axis. They consist of “half” strips that cover only half of the angular distance of the detector and have a strip pitch of $40\ \mu\text{m}$. The next section covers the distance to 2.8 cm on the detector. Again the strip pitch is $40\ \mu\text{m}$, however in this section the strips cover the full angular distance of the detector. The final section is comprised of full strips with a pitch of $60\ \mu\text{m}$ and runs from 2.8 cm to the end of the active area of the detector.

The Φ measuring detector consists of only two regions (figure 2). Unlike the R detector the strip pitch is not constant over the strip’s length and there is also a 5° stereo angle. In the inner region of the detector (up to 2.8 cm) the strip pitch varies from $45\ \mu\text{m}$ to $126\ \mu\text{m}$. From 2.8 cm to the end of the active area the pitch varies from $44\ \mu\text{m}$ to $79\ \mu\text{m}$.

2.2 The Test-Beam Telescope

The detector telescope used in the 1999 Autumn test-beam is similar to that used in the previous year. However, six of the previously used detectors removed. Detectors were removed from one side, essentially leaving the telescope with a row of detectors, three R measuring and three Φ measuring, equipped with VA2 readout electronics.

A diagram showing a schematic layout of telescope can be found in figure 3. It shows the pairs of detectors (one R measuring detector and one Φ measuring detector separated by a distance of the order of a few mm) with a distance of approximately 4cm between

each pair, as consistent with the design of the Technical Proposal [1]. The centre pair of detectors has been flipped by 180° to take full advantage of the Φ stereo angle.

3 VELO Test-Beam Analysis Code

All the analysis described below has been executed using the LHCb VELO test beam software (for a more detailed description see [2]).

The software is based around the `ROOT` framework and makes full use of its many features. Data is stored in `ZEBRA FZ` files and is converted to a `ROOTDB` within the `VELOROOT` analysis code and returned in the form of a `ROOT` output file. The global frame of reference is defined relative to the R and Φ measuring planes of the detectors, where the z axis is in the direction of the beam. Track fitting is performed by the `TestBeamTrack` class in the `VELOROOT` software. The trackfit takes a `ClusterSet` (a minimum of 6 clusters, one per detector, is required) and iteratively finds the track with the lowest χ^2 through each detector. Further details of how this algorithm works can be found in [2] or [3].

The detectors within the telescope were aligned using the `MINIMIZE` method in `TMinuit`. First, a “fast track fit” together with the alignment class is used to fix the first R detector and the z position of the second R detector. `Minuit` is then run with 30 free parameters until a set of alignment constants is found. There are 6 alignment constants utilised in the `VELOROOT` code. Three account for displacements along the x , y and z axes, measured in cm. Alpha accounts for a rotation in the z axis, beta the y' axis rotation and gamma the x'' axis rotation. Each are measured in radians.

For a full alignment, two alignment files are required, `FLIP` and `ROTATE`. `FLIP` is needed to specify the rotations necessary to put the detectors in their nominal positions in the xy plane. `ROTATE` gives the small angular deviations and linear displacements necessary. Generally it is only the latter that is altered by software alignment.

The `ROOT` output files, as produced by the software, contain all histograms necessary for an analysis, from basic cluster level histograms to those used in more complex analyses. The majority of histograms shown below have been produced in this manner.

4 Telescope Resolution

4.1 Experimental Procedure

Both the test-beam telescope and detectors under study were tested in 120GeV/c muon test-beam in the CERN SPS. They were sealed in a darkened box which was connected to a cooling pump, necessary to simulate real working conditions, particularly for the irradiated detector present. Approximately midway through the beam run period an air blower was added to the set-up as it was suspected that the low temperature was the cause of low gain on the first/last channels of the VA2 chips.

The main purpose of the telescope in this beam test was to provide the reconstructed tracks to be used in analysing data for the detectors under study (in this case an irradiated DELPHI module and an irradiated LHCb R detector fitted with SCTA readout electronics). The two scintillators also present provided the trigger due to particles crossing the test beam setup. To ensure that good quality data were provided for analysis of

the detectors under study, a full understanding of the operation of the telescope is needed. The remainder of this note provides a description of the study of the spatial resolution of the R and Φ detectors with the test-beam telescope.

4.2 Analysis

To ensure high quality data, a systematic study was therefore made of the track fit residuals for each region of each detector. Here the residual is defined as being the difference between the reconstructed track and cluster centre as given by the software described in section 3. For the R/Φ detectors respectively, plots were made of the residual distribution with respect to R and Φ for each region of the detector (figures 1 and 2) and for each possible combination of regions within the telescope. The combinations are defined as the region in detector for each subsequent detector in the telescope, i.e. R,Φ,R,Φ,R,Φ . For example combination 1,0,0,0,1,0 corresponds to a track through the inner regions of each detector in the telescope (see figure 3). Since there are a considerable number of combinations with very few or zero entries, a minimum number of 50 entries was set to produce a distribution of means with respect to combination of regions (see figure 6). The mean of this plot for a well aligned telescope should be zero and figure 6 clearly shows that this is the case. For some combinations of regions small offsets are seen, although these are by no means in the majority. Investigations into which regions cause such offsets found that a small percentage are difficult to obtain physically and could become a subject of further study.

Shifts due to environmental changes were also investigated. Among the most notable was perhaps the change in temperature due to the hot air blower. Large statistic studies of before and after show that the residuals produced are consistent within experimental error (see figures 4 and 5). It was also necessary to investigate the quality and stability of the telescope alignment. Figures 7 and 8 show that no correlation can be seen between the distribution of residual means with respect to run number. Here the mean is that given by the Gaussian fit. Figure 9 shows the total and projected angle at which the track hits the telescope. When compared to a track that hits straight vertical strips perpendicularly, the projected angle is the angle at which the track moves to affect the charge sharing on the strips. The non-linearity of the strips has been accounted for when finding this angle. It is found to be less than 2° for all regions of all detectors, although for the R it is actually 0.4° .

4.3 Intrinsic Spatial Resolution

To determine the spatial resolution of each detector, single Gaussian fits were made to the projected residual distributions of the detectors in the telescope. These were found for each region of the detectors as well as each possible combination of regions for systematic studies. It can be shown that for three detectors, equally spaced, the true resolution is equal to the scaled width of the residual distribution. For the middle detector in the telescope, the residual width is divided by $\sqrt{2/3}$. This factor is $\sqrt{1/6}$ for the outer detectors. This is true only for the special case of equal z-spacing.

Figure 10 shows the projected residual distribution for the area covered by strips with a $40\ \mu\text{m}$ pitch (left-hand side) and the $60\ \mu\text{m}$ region (right-hand side) of the R detector.

For the 40 μm regions of the central R detector (detector 4 in the plots) a residual width of 5.5 μm gives a spatial resolution of $(6.8 \pm 0.1) \mu\text{m}$. This compares well with the outer detectors, giving resolutions of 6.2 μm and 7.4 μm .

The residual width of the 60 μm region of the same central R detector is 9.4 μm and thus gives a resolution of $(11.5 \pm 0.1) \mu\text{m}$. Again a reasonable comparison can be made with the detectors 2 and 6, having resolutions of 10.7 μm and 13.1 μm respectively.

Theoretically, it can be shown that the resolution of a microstrip detector is related to the pitch by

$$\sigma = \frac{pitch}{x * \sqrt{12}} \quad (1)$$

where x is a factor taking into account the greater detail present due to charge sharing with analogue readout as compared to no charge sharing as with digital readout. For digital readout, this factor is one.

For a pitch of 40 μm , this factor is 1.8 for an R measuring VELO which suggests that there is a large amount charge sharing. Using this value of x and equation 1 a value for the resolution of a 60 μm pitch detector was found to be 9.7 μm . This is less than the value found from the test-beam data, suggesting that there is less charge sharing at a greater pitch. Consistent with this, a value of $x = 1.5$ was found using the data from the 60 μm regions of the detectors in the telescope.

As described in section 2.1, the pitch of a Φ measuring detector varies with radius thus a relationship between pitch and resolution is required. For each of the regions of the detector a histogram of track residual (in cm) as a function of pitch was plotted. The pitch was then divided in sections and a Gaussian fitted to the residual projection of each "slice". Histograms of the means and widths of these fits were plotted and the subsequent minimum χ^2 fit leads to a relationship of the form:

$$f(x) = p0 + p1 * x \quad (2)$$

Figure 12 shows that for the inner region of the detector, where the pitch varies from 45 μm to 126 μm , the resolution varies as:

$$resolution = (0.23 \pm 0.01) * pitch - (4.6 \pm 0.9) \quad (3)$$

Similarly for the outer region, where the pitch varies from 44 μm to 79 μm ,

$$resolution = (0.21 \pm 0.01) * pitch - (3.4 \pm 0.4) \quad (4)$$

Although not necessarily expected, straight line fit gives a good relationship between pitch and resolution to first order. Thus using relationships 3 and 4, predictions for the resolution at inner and outer most points of each region can be made. These are shown in table 1.

Detector	Pitch (μm)	Resolution (μm)	x
Φ : Inner region	45	5.8 ± 0.5	2.2 ± 0.2
Φ : Inner region	126	24.6 ± 1.4	1.5 ± 0.1
Φ : Outer region	45	5.8 ± 0.5	2.2 ± 0.2
Φ : Outer region	79	12.8 ± 0.7	1.8 ± 0.1
R : Inner region	40	6.8 ± 0.1	1.7 ± 0.2
R : Outer region	60	11.5 ± 0.1	1.5 ± 0.1

Table 1: Table of resolutions.

Pitch (μm)	TP (μm)	R (μm)	Φ (μm)
40	6	6.8 ± 0.1	5.3 ± 0.2
60	-	11.5 ± 0.1	10.4 ± 0.3
80	10	15.4 ± 0.1	15.4 ± 0.3

Table 2: Table of Resolutions, predicted values for $80\mu\text{m}$ to compare with those given in the Technical proposal (TP).

5 Conclusions and the Future

The results presented here show that, for the beam telescope used in the Autumn 99 test-beam, a comparison can be made with resolutions that are given in the Technical Proposal. Values for the $40\mu\text{m}$ and $80\mu\text{m}$ regions of the prototype R detector are given to be, for double (single) hit clusters, $6\mu\text{m}$ ($9\mu\text{m}$) and $10\mu\text{m}$ ($18\mu\text{m}$) respectively. The Level-1 - Level-3 triggers require the vertex detector to be aligned to a precision better than the reconstructed cluster position of $6\mu\text{m}$ [1].

From equation 1, a value for the resolution of an $80\mu\text{m}$ pitch detector such as that found described in the LHCb Technical Proposal may be found. Table 2 gives a prediction using a value of $x = 1.5$ i.e. that obtained from the $60\mu\text{m}$ region of the R detector. Figure 13 consolidates the results described in section 4.3. From this plot a general relationship between pitch and resolution for an LHCb-VELO detector may be obtained.

$$resolution = (0.254 \pm 0.003) * pitch - (4.9 \pm 0.1) \quad (5)$$

Again, it is not expected that this relationship be exactly linear, however relationship 5 gives resolutions that are good to first order. It is also worth noting that the two filled circles at $40\mu\text{m}$ and $60\mu\text{m}$, corresponding to resolutions obtained for the R detectors, are consistent with values obtained from the Φ detectors. Using relationship 5 predictions for Φ detector resolutions comparable to those from the Technical Proposal may be made. These are shown in table 2.

From these results it is clearly seen that the predictions of the Technical Proposal are inaccurate at larger pitches.

6 Acknowledgements

The author would like to thank all those involved in the VELO test-beam program, in particular Hans Dijkstra and Thomas Ruf. A special mention must also go to Paula Collins, Chris Parkes and David Steele for their invaluable assistance and support during this analysis.

References

- [1] The LHCb Collaboration. *Technical Proposal for A Large Hadron Collider Beauty Experiment for Precision Measurements of CP Violation and Rare Decays*. CERN/LHCC98-4, LHCC/P4 (20. 2. 1998).
- [2] C. Parkes. *Vertex Locator Test-Beam Software Description* LHCb/2000-096.
- [3] <http://lhcbproject.web.cern.ch/lhcbproject/velo/testbeam/Welcome.html> - online description of VELOROOT software.
- [4] LHCb TestBeam Group *VELO Telescope Resolution and Efficiency Measurements* LHCb-VELO/2000-99.

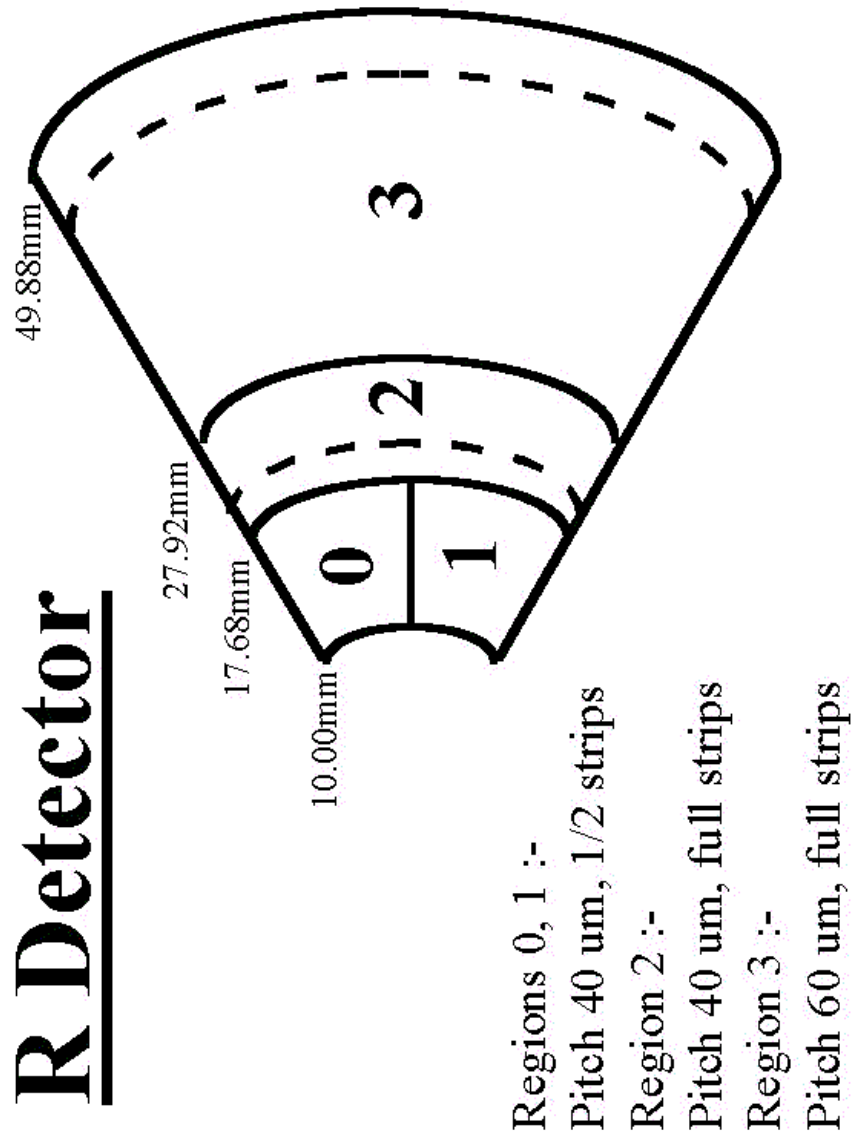


Figure 1: A Schematic layout of the detector regions in the *R* Detector, dashed lines show strips.

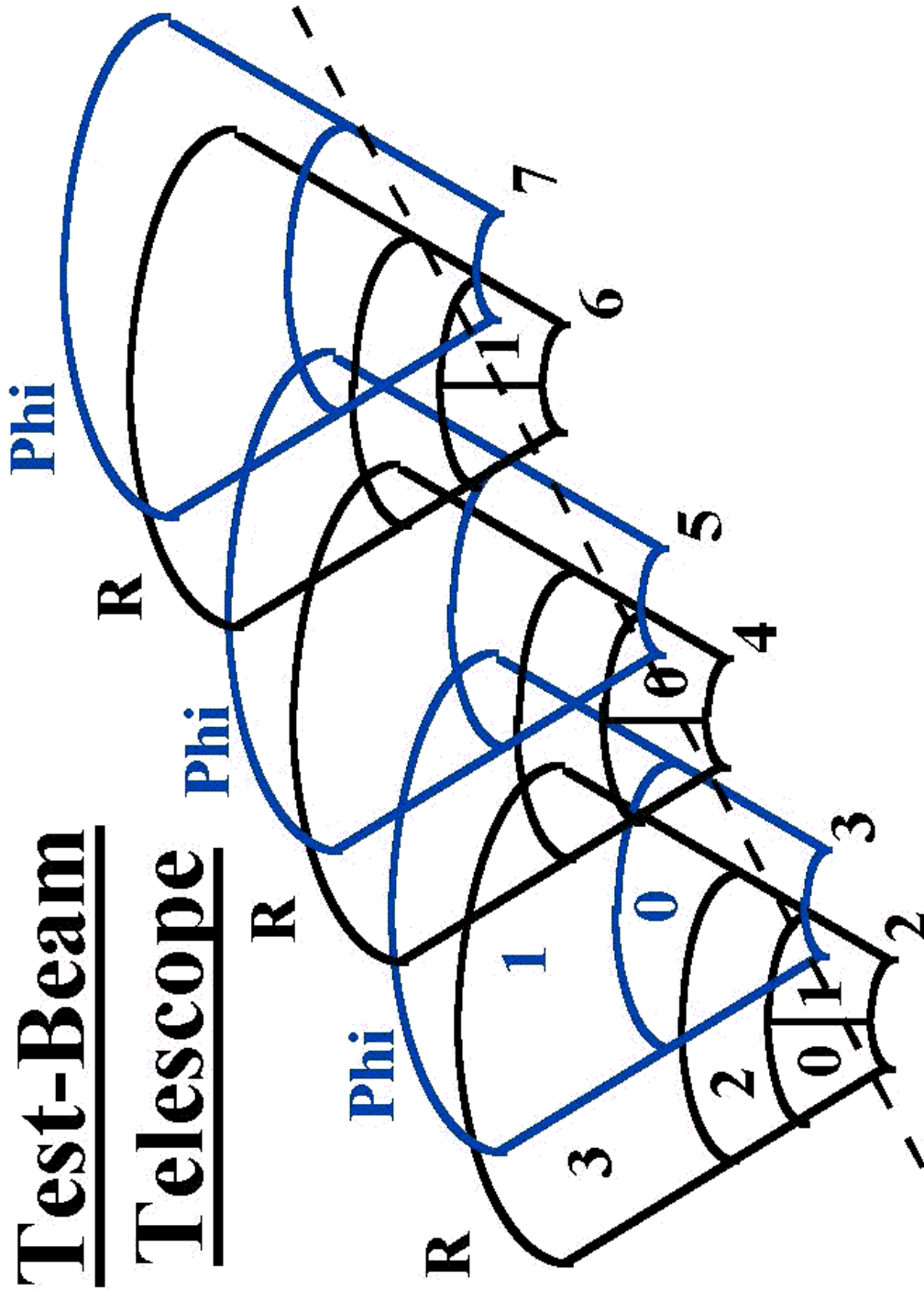


Figure 3: A Schematic Layout of the Test-Beam Telescope used in the Autumn 1999 Test-Beam. Dashed line shows the position of the track for combination of region 1,0,0,0,1,0.

TrackFit Residuals R Detector 2 and Regions 3,3,3,1,1,1

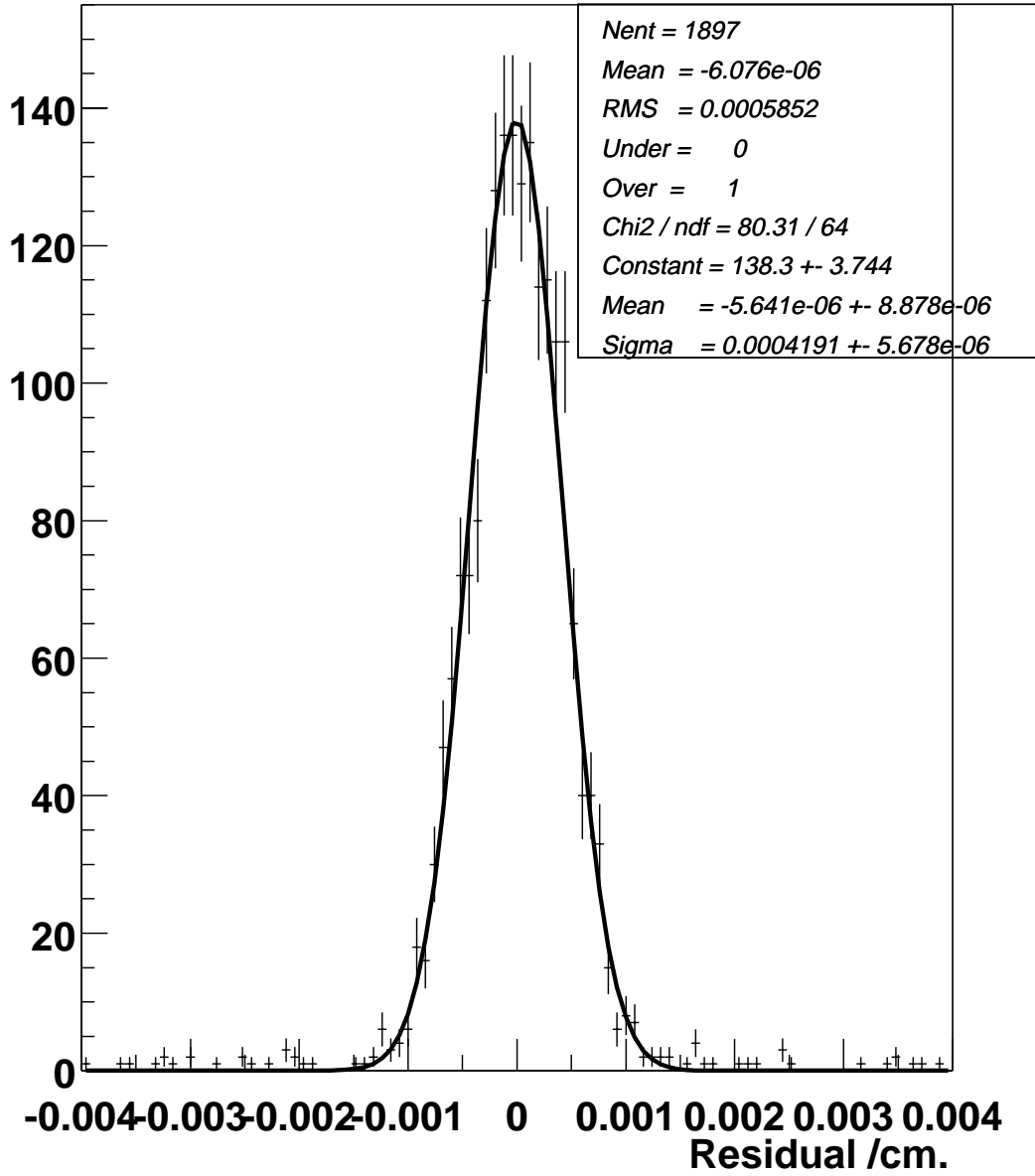


Figure 4: Track residuals for one R detector and one combination of regions for those runs before the air blower was switched on.

TrackFit Residuals R Detector 2 and Regions 3,3,3,1,1,1

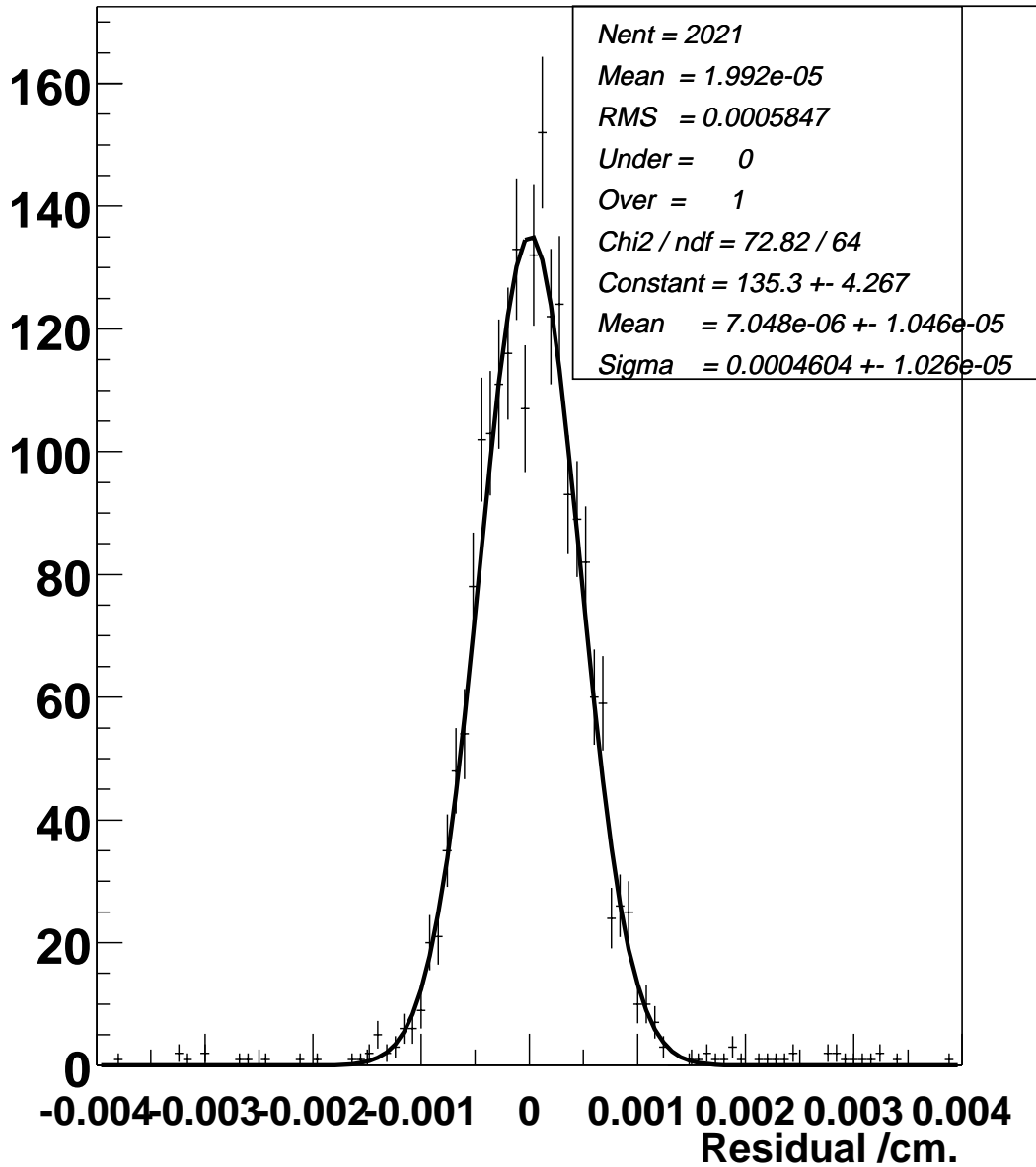


Figure 5: Track Residuals for one *R* detector after the air blower had been switched on. A comparison between this and figure 4 shows that switching on the air blower had little effect on the resolution of the detectors.

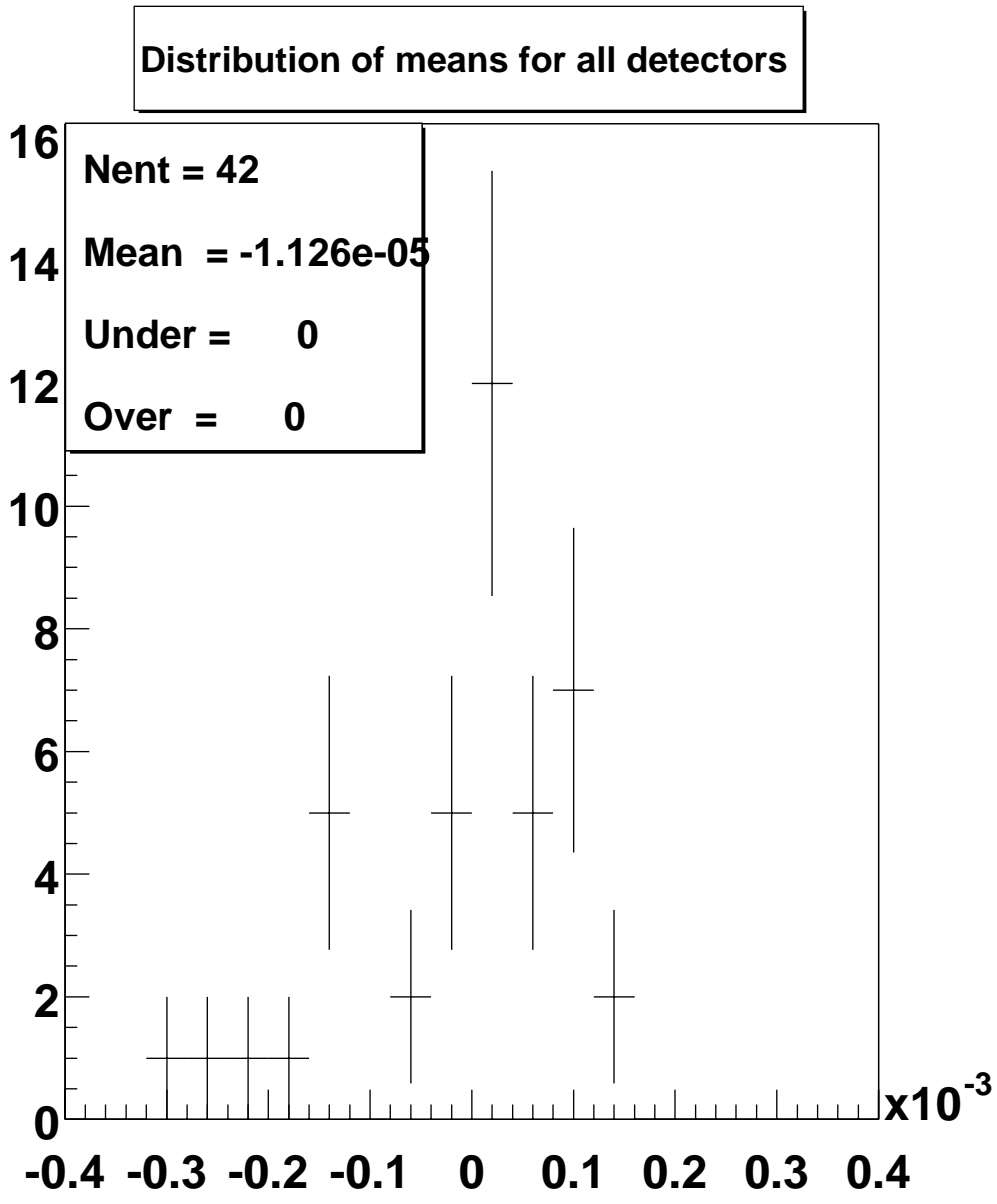


Figure 6: Distribution of residual means (cm) with respect to combination of region. A mean of 0.1 μm suggests that the detectors are reasonable well aligned within the telescope.

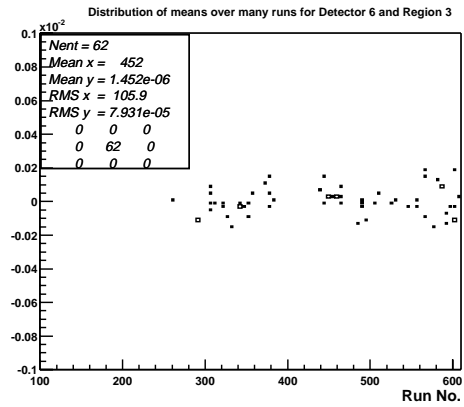
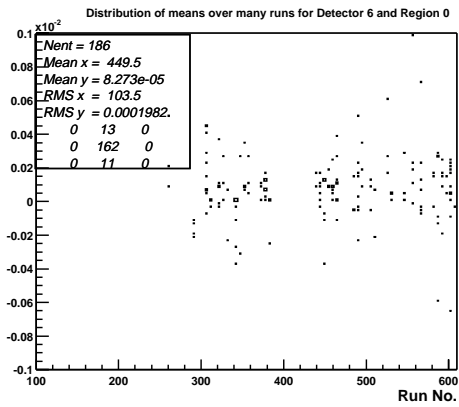
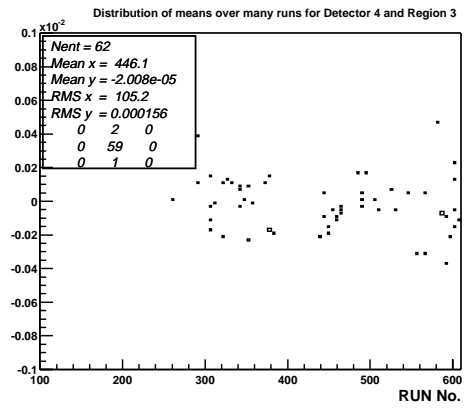
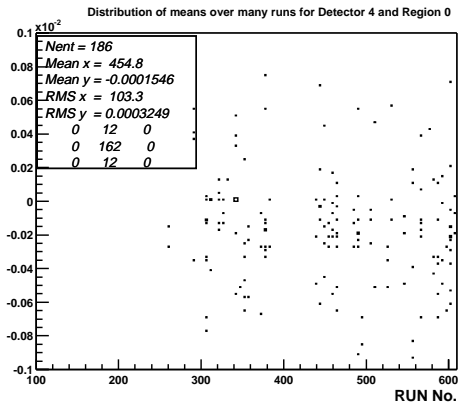
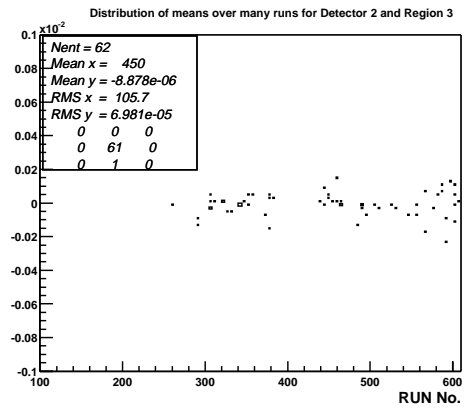
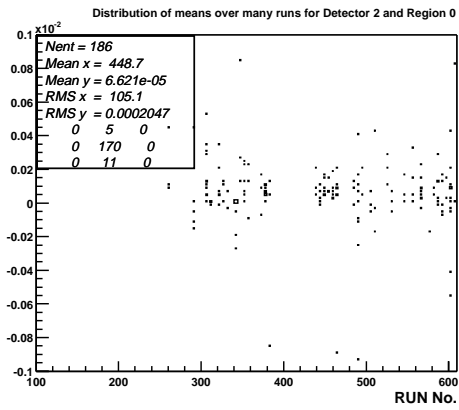


Figure 7: Distribution of means (cm) over many runs for the inner regions (left) and outer (right) of each R detector.

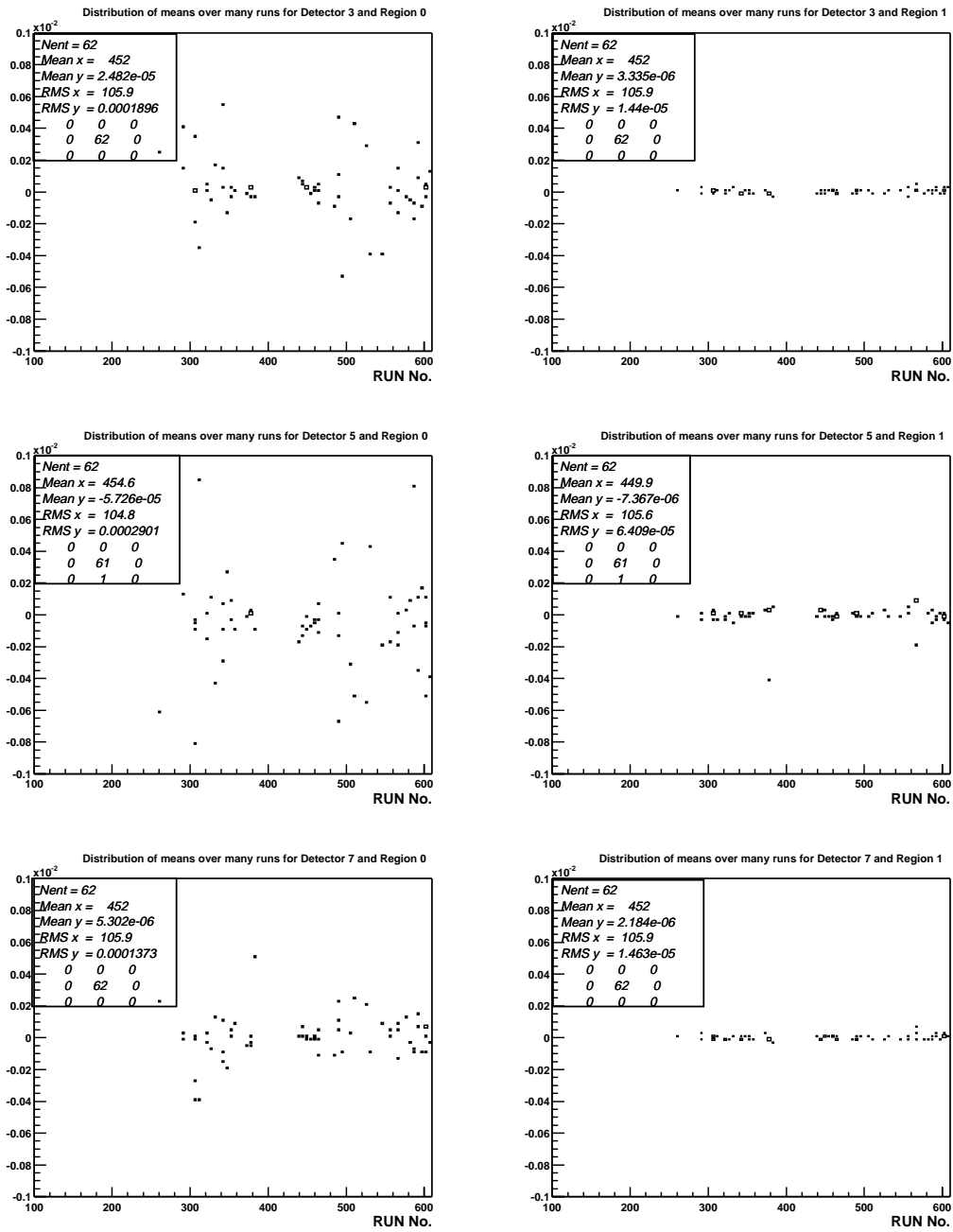


Figure 8: Distribution of means (cm) over many runs for the inner regions (left) and outer (right) of each Φ detector.

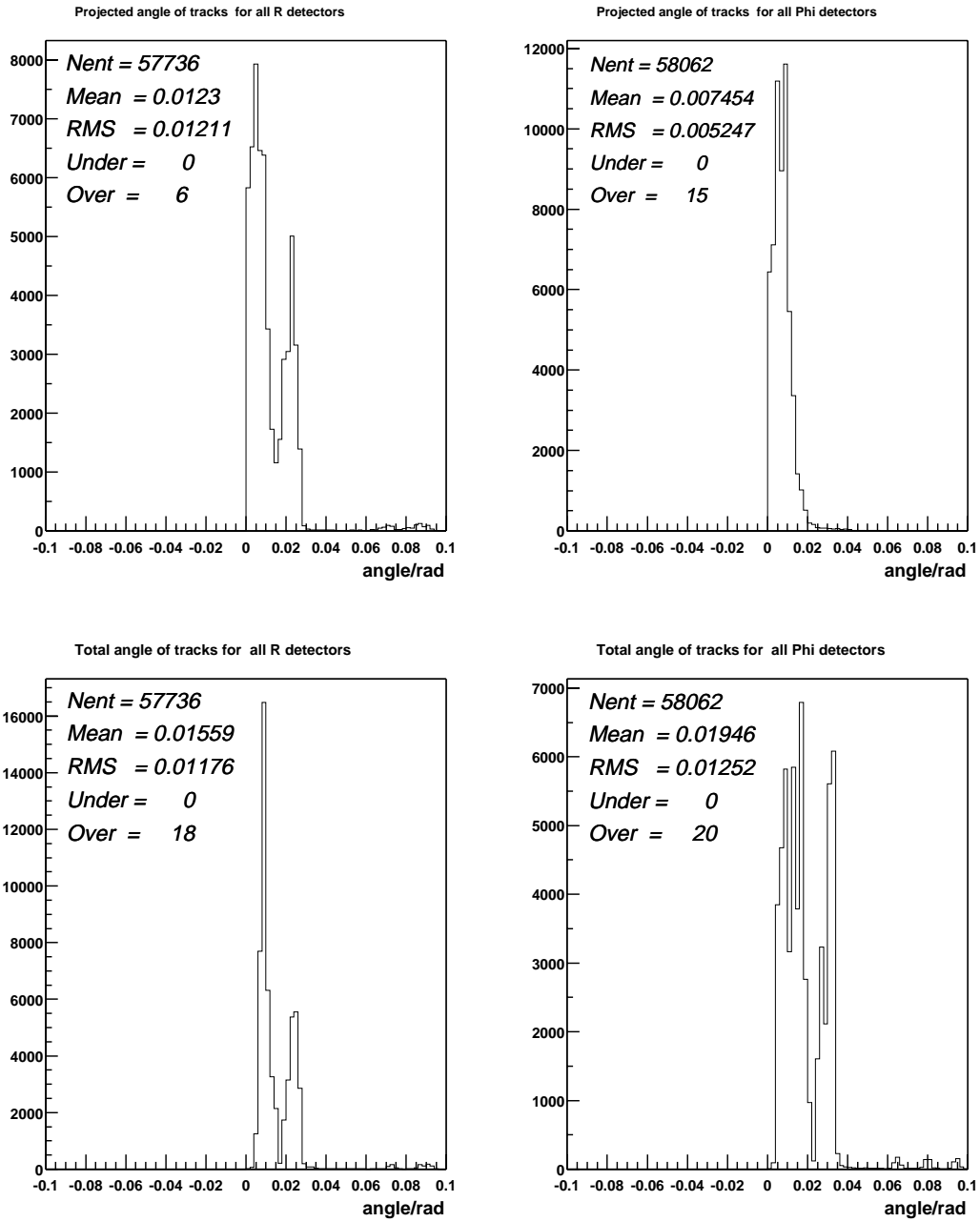
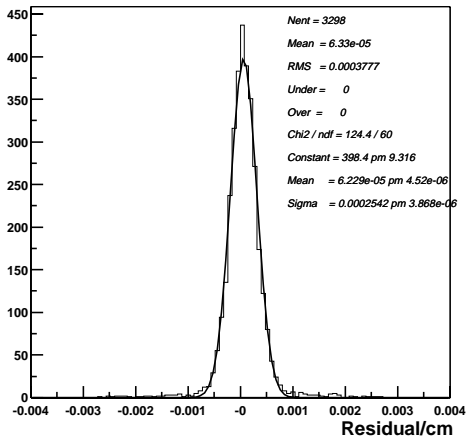
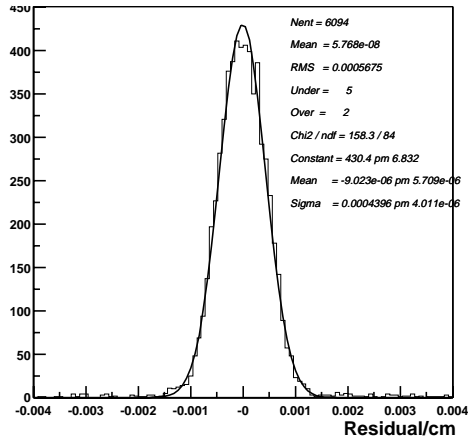


Figure 9: Projected (top) and Total (bottom) Angle of Tracks for R (left) and Φ (right) Detectors. All angles are within 2° .

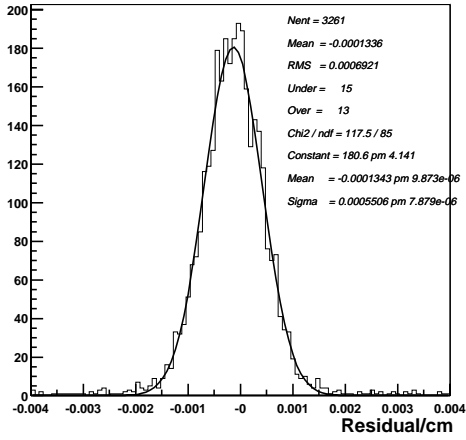
TrackFit Residuals Detector 2 and Region 0



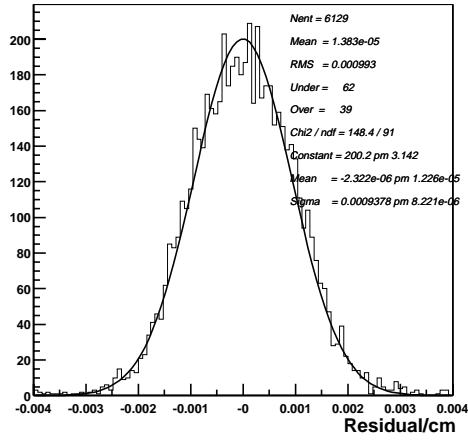
TrackFit Residuals Detector 2 and Region 3



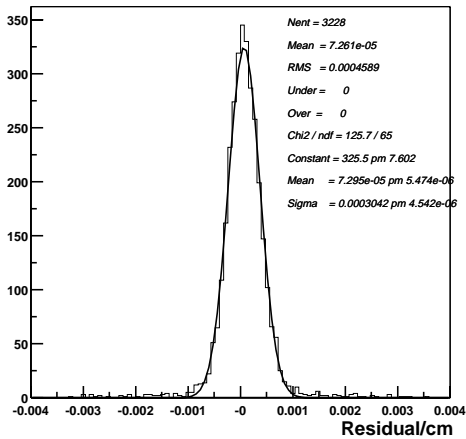
TrackFit Residuals Detector 4 and Region 0



TrackFit Residuals Detector 4 and Region 3



TrackFit Residuals Detector 6 and Region 0



TrackFit Residuals Detector 6 and Region 3

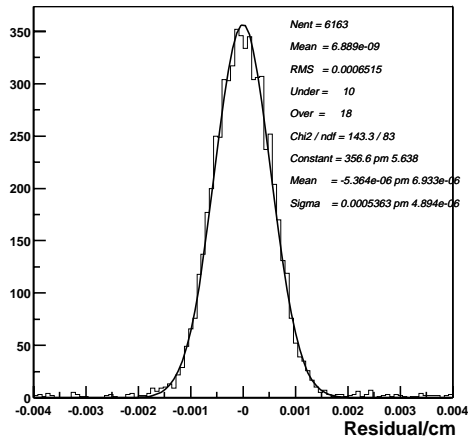


Figure 10: Track Residuals for the inner (left) and outer (right) regions of the R detector.

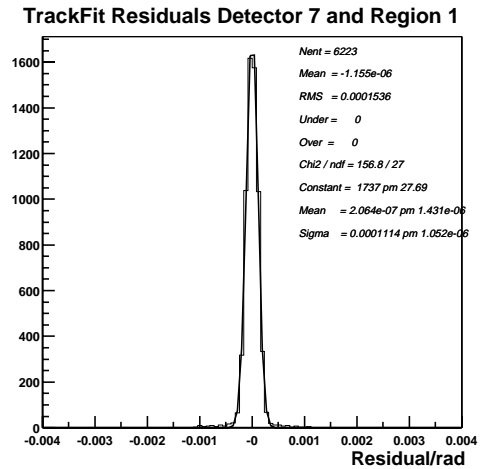
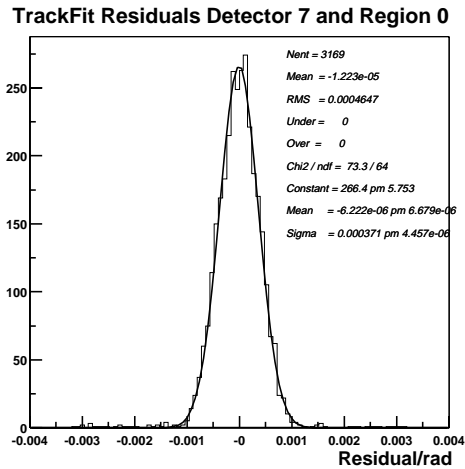
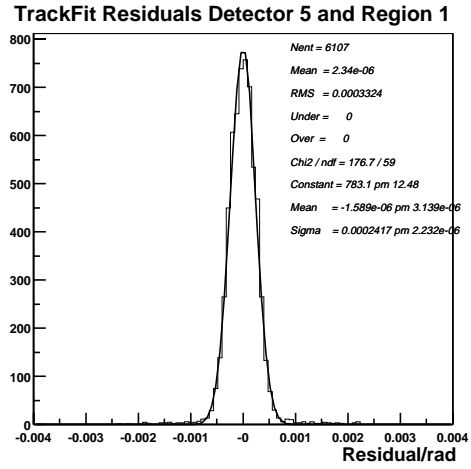
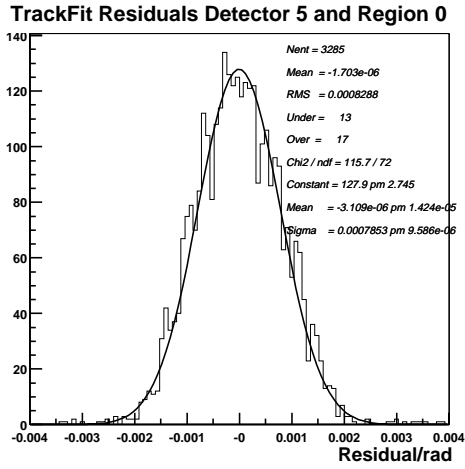
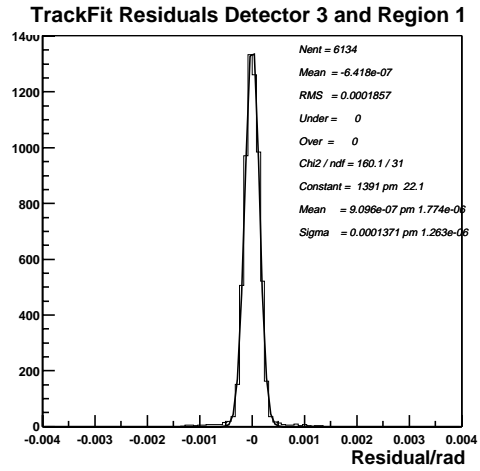
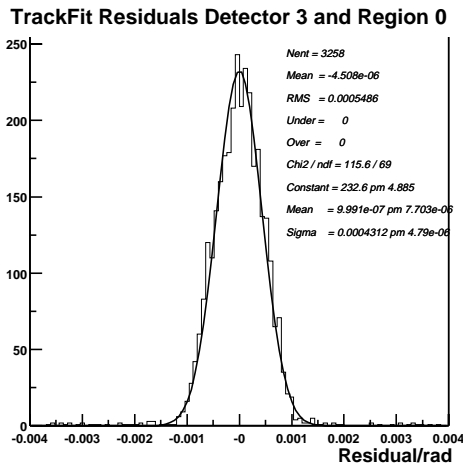


Figure 11: Track Residuals for the inner (left) and outer (right) regions of the Φ detector.

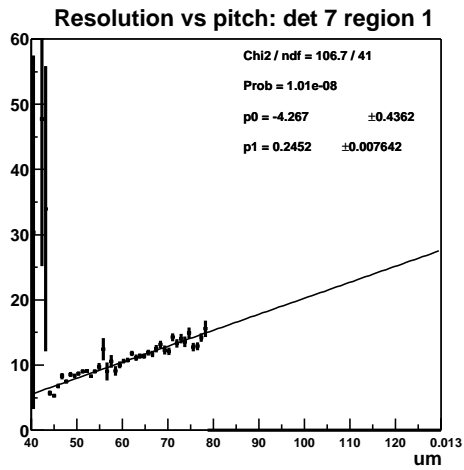
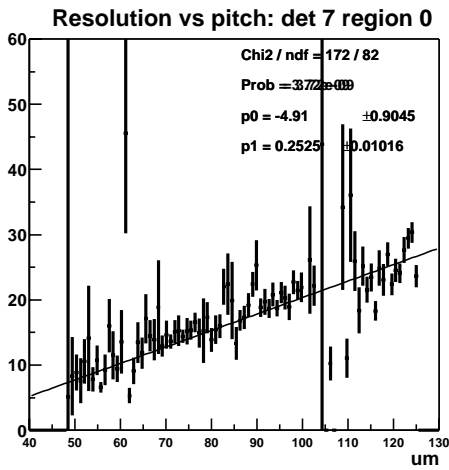
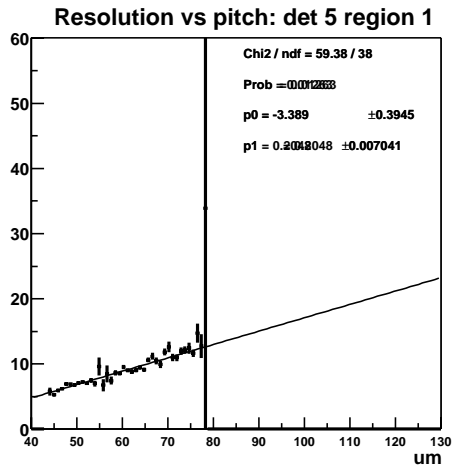
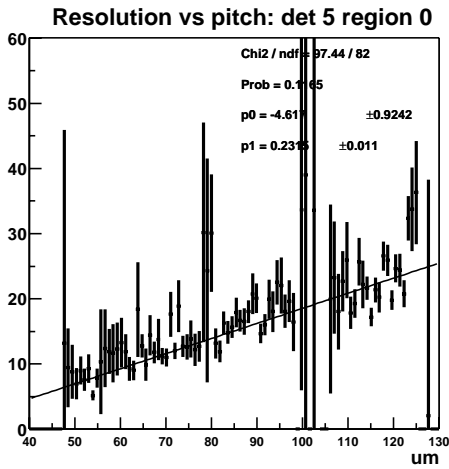
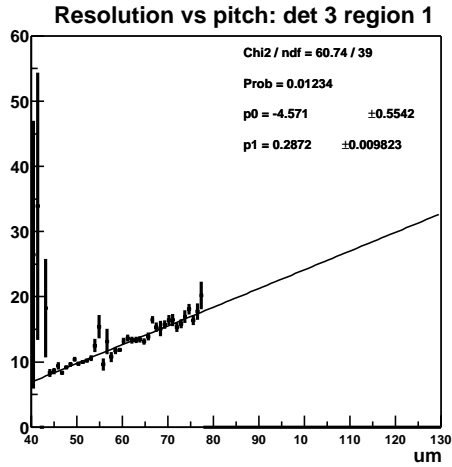
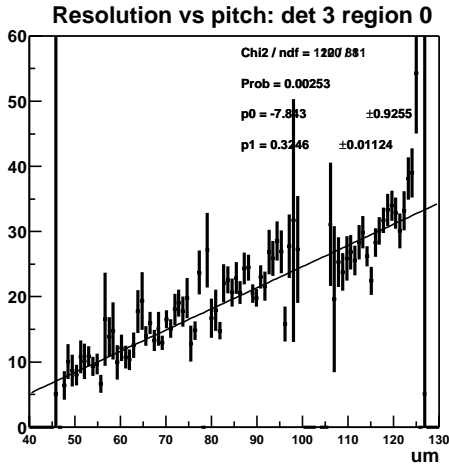


Figure 12: Variation of the resolution of a Φ detector as a function of pitch for the inner (left) and outer (right) regions.

Resolution vs pitch: all detectors

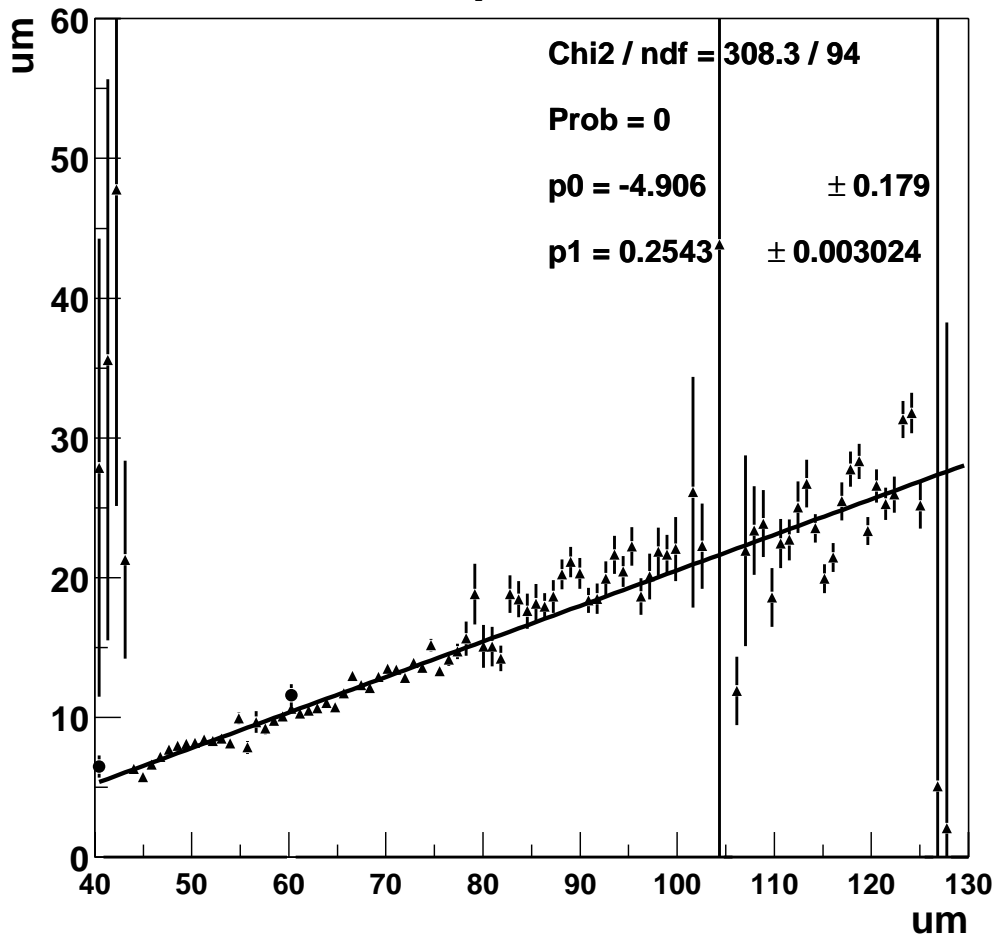


Figure 13: Variation of the Resolution as a Function of Pitch for all detectors. Circles: R detector resolutions. Triangle: Φ detector resolutions.